pharmaceutics

MDPI

Article

The Anti-Inflammatory Effect of Nanoarchaeosomes on Human Endothelial Cells

Nancy Charó [1], Horacio Jerez [2], Silvio Tatti [3], Eder Lilia Romero [2,*] and Mirta Schattner [1,*]

[1] Laboratory of Experimental Thrombosis and Immunobiology of Inflammation, Institute of Experimental Medicine, CONICET-National Academy of Medicine, Pacheco de Melo 3081, Buenos Aires 1425, Argentina; nancycharo@hotmail.com
[2] Center for Research and Development in Nanomedicines (CIDEN), National University of Quilmes, Roque Saenz Peña, Bernal 1876, Argentina; jairjerez@gmail.com
[3] Department of Obstetrics and Gynecology, Clinical Hospital, Av. Córdoba 2351, Buenos Aires 1120, Argentina; drestatti@gmail.com
* Correspondence: elromero@unq.edu.ar (E.L.R.); mschattner@hotmail.com (M.S.)

Abstract: Archaebacterias are considered a unique source of novel biomaterials of interest for nanomedicine. In this perspective, the effects of nanoarchaeosomes (ARC), which are nanovesicles prepared from polar lipids extracted from the extreme halophilic *Halorubrum tebenquinchense*, on human umbilical vein endothelial cells (HUVEC) were investigated in physiological and under inflammatory static conditions. Upon incubation, ARC (170 nm mean size, −41 mV ζ) did not affect viability, cell proliferation, and expression of intercellular adhesion molecule-1 (ICAM-1) and E-selectin under basal conditions, but reduced expression of both molecules and secretion of IL-6 induced by lypopolysaccharide (LPS), Pam3CSK4 or *Escherichia coli*. Such effects were not observed with TNF-α or IL-1β stimulation. Interestingly, ARC significantly decreased basal levels of von Willebrand factor (vWF) and levels induced by all stimuli. None of these parameters was altered by liposomes of hydrogenated phosphatidylcholine and cholesterol of comparable size and concentration. Only ARC were endocytosed by HUVEC and reduced mRNA expression of ICAM-1 and vWF via NF-kB and ERK1/2 in LPS-stimulated cells. This is the first report of the anti-inflammatory effect of ARC on endothelial cells and our data suggest that its future use in vascular disease may hopefully be of particular interest.

Keywords: nanoarchaeosomes; endothelium; inflammation; ICAM-1; von Willebrand factor; nanovesicles

Citation: Charó, N.; Jerez, H.; Tatti, S.; Romero, E.L.; Schattner, M. The Anti-Inflammatory Effect of Nanoarchaeosomes on Human Endothelial Cells. *Pharmaceutics* **2022**, *14*, 736. https://doi.org/10.3390/pharmaceutics14040736

Academic Editor: Tomáš Etrych

Received: 22 February 2022
Accepted: 24 March 2022
Published: 29 March 2022

1. Introduction

In the last 25 years, nearly 60 therapeutic nanomedicines entered the pharmaceutical market, while a growing number are in advanced clinical trials [1], most of them aimed to target solid tumors upon intravenous administration [2]. The recent approval by the FDA of Patisiran/Onpattro, a novel nanomedicine for efficient RNA delivery to the liver [3], has paved the way for the fast advent of new nanoparticulate anti-COVID-19 vaccines, such as those from Moderna and Pfizer [4]. However, despite cardiovascular disease being the primary cause of global mortality (31% of all deaths worldwide) [5], the evolution of cardiovascular nanomedicines is still in its childhood [6]. Research in this area consists of proof-of-concept nanomedicines targeted to the vascular endothelium and neighbouring cells to deliver anti-inflammatory or anti-proliferative agents [7]. The endothelium is a key target for therapeutic interventions in several conditions. It represents an enormously extended surface area accessible to blood (3000–6000 m^2) [8], and is not only critical for the maintenance of vascular function and homeostasis, but it is also sensitive to the chemical nature of nanoparticles (NPs) in the bloodstream. In fact, endothelial injury or dysfunction is the initial cause of atherosclerosis and other cardiovascular diseases [9]. For instance, endothelial cells are sensitive to the chemical nature of metallic and metallic

oxide NPs. ZnO, silica, and Ag NPs activate human endothelial cells through the NF-κB pathway [10–13]. Gold NPs, however, are less harmful to endothelial cells, and have been employed in the identification of plaques and the recognition of inflammatory markers [14].

The endothelium, on the other hand, seems to be inert to the interaction with biodegradable polymer NPs, micelles, and liposomes conforming to the core of most therapeutic and prophylactic nanomedicines [15,16]. New materials of a heterogeneous chemical nature, such as inorganic-organic hybrids, whether bio-inspired [17], or of natural origin, are increasingly enriching the architecture of novel preclinical nanomedicines, but whose effect on the vascular endothelium are still not completely clear. Nanoarchaeosomes (ARC), for instance, are nanovesicles in current preclinical exploration as drug and vaccine nanocarriers, consisting of closed bilayers made of amphipathic archaeolipids isolated from extreme halophiles, methanogens or extreme thermophile archaebacteria [18–23]. The nature of the hydrophilic headgroups and the hydrophobic fully saturated chains of polar archaeolipids depend on the archaebacteria genus [24], meaning that the term ARC encompasses nanovesicles of variable structural composition. Different from phospholipids from Eukarya and Bacteria domains, the amphipathic archaeolipid possesses an sn-2,3 stereoisomerism, and a glycerol backbone ether-linked to fully saturated polyisoprenoid chains. Such unique chemical structure makes ARC refractory to enzymatic attacks, hydrolysis and oxidation [25], cold chain interruption during transport and storage [26], and resistant to nebulization shear stress [27]. Archaebacteria's lack of lipopolysaccharide (LPS) and ARC from different sources showed to be non-toxic or mildly toxic in in vitro and in vivo conditions [28]. Because of these reasons, ARC are interesting alternatives to liposomes, are less labile, and have extended structural benefits. For example, we have recently reported that ARC from *Halorubrum tebenquichense* (*H. tebenquichense*) loaded with dexamethasone or curcumin display repairing activity on inflamed intestinal and lung epithelia [29,30]. The specific composition of *H. tebenquichense* ARC was determined by electrospray-ionization mass spectrometry (ESI-MS) [31] and ordered according to decrescent abundance as archaeol analog methyl ester of phosphatidylglycerol phosphate (PGP-Me), archaeol analog phosphatidylglycerol (PG), (1-O-[a-D-mannose-(2′-SO3H)-(1′ a 2′)-a-D-glucose]-2,3-di-O-phytanyl-sn-glycerol) (SDGD5) the cardiolipin bis phosphatidylglycerol (BPG) and the glycocardiolipin SDGD-5PA (2′-SO3H)-Manp-a1,2Glcpa-1-1-[sn-2,3-di-O-phytanylglycerol]-6-[phospho-sn-2,3-di-O-phytanylglycerol]. Until now however, there are no reports about the interaction of these ARC with endothelial cells. We present here the first assessment of ARC uptake by human endothelial cells under physiological and inflammatory conditions.

2. Materials and Methods

Hydrogenated soy phosphatidylcholine (HSPC) was purchased from Northern Lipids Inc (Vancouver, BC, Canada). Cholesterol was from ICN Biomedicals. Lissamine™ rhodamine B 1,2-dihexadecanoyl-sn-glycero-3-phosphoethanolamine triethylammonium salt (RhPE) was obtained from Thermo Fisher Scientific (Waltham, MA, USA). Yeast extract was from Laboratorios Britania S.A. (Buenos Aires, Argentina). Purified LPS derived from *Escherichia coli* (*E. coli*) O111:B4, phorbol 12-myristate 13-acetate (PMA), and Ionomycin were purchased from Sigma (Burlington, MA, USA). Pam3CysSerLys4 (Pam3CSK4) and polyinosinic: polycytidylic acid (Poly (I: C)) were from InvivoGen (San Diego, CA, USA). Recombinant Human Tumor Necrosis Factor-alpha (TNF-α) was purchased from Cell Signaling Technology (Beverly, MA, USA). Interleukin (IL)-1β and Click-iT® Plus EdU Alexa Fluor-488, were obtained from Invitrogen (Carlsbad, CA, USA). *E. coli* DH5a was a kind gift from Dr. Ricardo Gomez (Biotechnology and Molecular Biology Institute, CONICET-UNLP, La Plata, Argentina). The other analytic grade reagents were from Anedra, Research AG (Buenos Aires, Argentina).

2.1. Archaebacteria Growth, Extraction & Characterization of Total Polar Archaeolipids

H. tebenquichense, archaea isolated from soil samples collected from Salina Chica, Peninsula de Valdés, Chubut, Argentina were grown in basal medium supplemented with yeast extract and glucose at 37 °C [19]. Biomass was grown in a 15 L medium in a 25 L homemade stainless-steel bioreactor and harvested after 96 h growth. Total polar archaeolipids (TPA) were extracted from the biomass using the method of Bligh and Dyer modified for extreme halophiles [32]. Between 400 mg and 700 mg of TPA was isolated from each culture batch. The reproducibility of each TPA-extract composition was routinely screened by phosphate content [33] and ESI-MS, as described in [31] (Supplementary Figure S1).

2.2. Preparation of Nanovesicles

Conventional liposomes made of HSPC: cholesterol 7.5:2.5 *w*/*w* (LIP), and nanoarchaeosomes made of TPA: cholesterol (7:3: *w*/*w*) of the extreme halophile archaea *H. tebenquichense* (ARC), were prepared by the film hydration method [34]. Total lipids were dissolved in chloroform: methanol 1:1 *v*/*v* and solvents were rotary evaporated at 40 °C until elimination. The lipid films were rinsed with N_2 and hydrated with 10 mM Tris-HCl buffer pH 7.4, 0.9% *w*:*w* NaCl up to a final concentration of 10 mg/mL total lipids. The suspensions were sonicated for 1 h with a bath-type sonicator 80 W, 80 KHz and extruded 10–15 times through polycarbonate filters with a pore size of 0.4 μm and 0.2 μm using a Thermobarrel extruder (Northern Lipids, Vancouver, BC, Canada). For the preparation of LIP, hydration, sonication, and extrusion were performed at 55–60 °C. To prepare RhPE-labeled nanovesicles, RhPE was added to the mixed organic solution of lipids at a rate of 0.4 μg per mg of lipids and the resultant lipid films were hydrated with a NaCl-Tris-HCl buffer as described above. All nanovesicles were sterilized by passage through a 0.22 μm sterile filter and stored at 4 °C.

2.3. Characterization of Nanovesicles

Total phospholipid content was quantified by colorimetric phosphate microassay [33]. RhPE was quantified by spectrofluorometry (λ_{ex} = 561 nm and λ_{em} = 580 nm) using a LS55 fluorescence spectrometer (PerkinElmer Inc., Waltham, MA, USA), after complete disruption of 1 volume of nanovesicles in 10 volume of methanol. The fluorescence intensity of the sample was compared with a standard curve prepared using RhPE in methanol. The standard curve was linear in the range of 0.075–0.5 μg/mL RhPE with a correlation coefficient of 0.999. The size and ζ potential of nanovesicles were determined by dynamic light scattering and phase analysis light scattering, respectively, using a Zeta nanosizer instrument (Malvern Instruments, Malvern, Worcestershire, UK).

2.4. Endothelial Cell Culture

This study conforms to the tenets of the Declaration of Helsinki and was previously approved by the institution's ethics committee. The umbilical cord was collected after normal deliveries with written informed consent from the mother. Human umbilical vein endothelial cells (HUVEC) were purified from human umbilical vein by digestion with collagenase (Gibco, Grand Island, NY, USA) according to the method of Jaffe et al. [35]. Cells were grown in a 2% gelatin (Sigma, St. Louis, MO, USA) coated plate with Endothelial Growth Medium-2 (EGM2) (Lonza, Lexington, MD, USA) supplemented with antibiotics (100 U/mL penicillin and 100 μg/mL streptomycin). HUVEC were used between the first and fourth passages. Human microvascular endothelial cells (HMEC) (ATCC Cell Lines) were maintained in MCDB 131 medium containing 15% *v*/*v* fetal bovine serum, hydrocortisone, and human epidermal growth factor human supplemented with antibiotics. Cells were incubated at 37 °C in a humidified atmosphere with 5% CO_2.

2.5. Measurement of Cell Viability and Apoptosis

HUVEC cultured in RPMI/1% FBS (Gibco) were treated in the absence or presence of increasing concentrations of nanovesicles, and cell viability was determined 24 h later.

Adherent cells were harvested with 0.25% trypsin and pooled with detached cells. Cells were then stained with a mixture of ethidium bromide and acridine orange (100 µg/mL), mounted on slides, and immediately analyzed by fluorescence microscopy. At least 300 cells per treatment were counted [36].

2.6. EdU Cell Proliferation Assay

HUVEC (2.5×10^4 cells) were plated in 48-well plates and incubated overnight at 37 °C to allow attachment. Cells were then incubated with ARC in EGM2 for 24 and 48 h. Subsequently, cells were incubated with 10 µM 5-ethynyl-2′-deoxyuridine (EdU) for 2 h. After incubation, cells were trypsinized, washed with phosphate buffered saline (PBS), and then stained with Alexa fluor 780 viability dye (eBioscience) at 4 °C for 30 min. Cells were fixed with 4% paraformaldehyde (PFA) for 15 min, washed once with bovine serum albumin/PBS buffer, permeabilized with a perm/wash buffer (BD Biosciences, San Jose, CA, USA), and treated with Alexa Fluor® 488 using the Click-iT® EdU Imaging Kit, washed, resuspended in buffer and analyzed by flow cytometry using a Sysmex-Partec CyFlow® Space. The percentage of proliferating cells that have incorporated EdU was defined within the viable cell population.

2.7. Expression of E-Selectin and ICAM-1

HUVEC were incubated with or without ARC and various stimuli. ICAM-1 expression was determined after 18 h by labelling cells in the dark with phycoerythrin (PE)-mouse anti-human CD54 (clone HA58, BD Pharmingen, San Diego, CA, USA). Because of the different expression peak ([37,38]), E-selectin was evaluated after 4 h HUVEC stimulation and then stained with a PE-anti-CD62E monoclonal antibody (Ab) (Clone 68-5H11, BD Pharmingen). To determine the nonspecific binding, cells were labeled with irrelevant isotype-matched IgG1 (Clone MOPC-21, BD Pharmingen). After labelling, cells were washed, fixed with 1% PFA, and then analyzed by flow cytometry.

2.8. Measurement of IL-6 and vWF

IL-6 was measured in the supernatant of the cells using an ELISA kit (eBioscience, San Diego, CA, USA). The concentrations of von Willebrand factor (vWF) in the supernatants were determined with a home-made ELISA using human vWF and horseradish peroxidase (HRP)-conjugated human vWF as primary and secondary Abs, respectively (Dako, Glostrup, Denmark). Results were expressed in ng/mL and extrapolated from serial dilutions of pooled normal plasma, assuming a vWF concentration of 7 µg/mL [39].

2.9. ARC Uptake by HUVEC

HUVEC (5×10^4 cells/well) were incubated with 50 µg/mL RhPE-labeled nanovesicles for various periods at 37 and 4 °C (control for nonspecific adsorption on the cell surface) and then trypsinized, washed, and analyzed by flow cytometry. The fluorescence of cells treated with ARC were corrected using the autofluorescence of untreated cells and the resulting data were analyzed using FlowJo 7.6 software. For confocal microscopy experiments, HUVEC were seeded on a glass coverslip and incubated with RhPE-labeled ARC for 4 h. Cells were then washed three times with cold PBS, fixed with 4% PFA, and stained with fluorescein IsoTioCyanate-phalloidin. After 3 washes, slides were inverted, mounted with PolyMount and analyzed by fluorescence microscopy using a FV-1000 microscope (Olympus, Tokyo, Japan).

2.10. Analysis of ERK1/2 and NF-κB Signaling Pathways

HMEC (2×10^5 cells/well) were cultured in complete medium and incubated overnight at 37 °C to allow attachment. HMEC were exposed to serum starvation for 2 h and then stimulated with LPS in the absence or presence of ARC. After incubation, endothelial cells were trypsinized, washed, fixed, and permeabilized as described in the BD Phosflow protocol (protocol III). Subsequently, cells were labeled with Abs against phospho-ERK1/2

(Tyr 202/Tyr 204) or IgG1κ isotype conjugated with Alexa Fluor® 488 and subjected to flow cytometry. NF-κB signaling was assessed by Western blotting. After starvation, HMEC were scraped and lysed with lysis buffer (60 mM de Tris/HCl, pH 6.8 + 1% SDS) in the presence of a cocktail of protease inhibitors (Sigma). After centrifugation, the lysates were electrophoresed and transferred to a nitrocellulose membrane. After blocking membranes were incubated with anti-phospho-ERK1/2 Santa Cruz Biotechnology, Santa Cruz, CA, USA) and anti-IκBα (BD Biosciences) followed by HRP-conjugated secondary Ab. Each membrane was reprobed with an Ab against β-actin (BD Biosciences) and proteins bands were visualized by ECL.

2.11. Quantitative PCR (qPCR)

HMEC were stimulated with LPS (1 μg/mL) with or without ARC for 18 h at 37 °C. Then, cells were washed and harvested with Trizol (Life Technologies, Carlsbad, CA, USA). Reverse transcription was performed using 100 ng of RNA and the iScript cDNA synthesis kit (Bio-Rad, Hercules, CA, USA). Real-time PCR reactions were determined using 1 μL cDNA and the SsoAdvanced universal SYBR Green mix and CFX-Connect equipment (Bio-Rad). The primers used are described in the Supplementary Table S1. The reaction was normalized to the expression levels of the housekeeping gene, and the specificity of the amplified products was verified by dissociation curves analysis.

2.12. Statistical Analysis

Results were reported as means ± SEM of independent experiments. The Shapiro-Wilk test was used to define the condition of normality and equal variance. Statistical differences between means were determined with Student's paired *t*-test or One-way ANOVA followed by Bonferroni multiple comparison tests using Graph Pad Prism version 6.00 (GraphPad Software Inc., San Diego, CA, USA). $p < 0.05$ values were considered statistically significant.

3. Results

3.1. Structural Characterization

The structural features (size, polydispersity index, ζ potential, total lipids, and RhPE) are shown in Table 1. Table 1 shows the structural features of the resulting nanovesicles, at concentrations between 7.5 ± 1.3 and 6.9 ± 0.6 for nanoARC and nanoARC-RhPE and 7.0 ± 1.7 and 6.0 ± 0.3 mg lipids/mL for LIP and LIP-RhPE, respectively. The nanoarchaeosomes exhibited a strong negative ζ potential, with mean diameters in the order of 160 nm, almost 100 nm smaller than those of liposomes. Both the nanoarchaeosomes and liposomes exhibited low PDI (≤0.3) and were labelled at a comparable ratio of RhPE/total lipids between 0.48–0.45 μg Rh-PE/mg TL.

Table 1. Physicochemical characteristics of nanovesicles.

Formulation	Size (nm ± SD)	PDI	ζ Potential (mV ± SD)	TL (mg/mL ± SD)	RhPE (μg/mL ± SD)	RhPE/TL (μg/mg ± SD)
ARC	168.9 ± 11	0.19 ± 0.01	−41.5 ± 4.5	7.5 ± 1.3	-	-
LIP	276.7 ± 11	0.30 ± 0.08	−5.4 ± 1.4	7.0 ± 1.7	-	-
ARC-RhPE	159.7 ± 7.6	0.19 ± 0.02	−37.0 ± 4.0	6.9 ± 0.6	3.2 ± 0.6	0.48 ± 0.09
LIP-RhPE	251.1 ± 9.1	0.29 ± 0.07	−3.7 ± 0.6	6.0 ± 0.3	2.8 ± 0.9	0.45 ± 0.12

Data are expressed as mean ± standard deviation from five independent batches (n = 3 for RhPE labeled nanovesicles). PDI: Polydispersity Index; SD: Standard Deviation; TL: total lipids.

3.2. ARC Do Not Alter HUVEC's Viability or Proliferation

Initially, we analyzed the effect of ARC on HUVEC viability and apoptosis by staining cells with ethidium bromide and acridine orange. As shown in Figure 1A, neither ARC nor liposomes affect the viability and apoptosis of HUVEC after 24 h incubation at concentrations up to 50 μg/mL. However, a statistically significant reduction in the cell viability and nuclear changes characteristic of apoptotic cells were observed in HUVEC treated with 100 μg/mL ARC (Figure 1A,B). Thus, in all the rest of the experiments, ARC and liposomes were used at 50 μg/mL. To determine whether ARC alter HUVEC growth, the cell cycle was evaluated by measuring the EdU incorporation. No differences in the thymidine analog incorporation were observed regardless of whether cells were exposed to nanovesicles or not (Figure 1C).

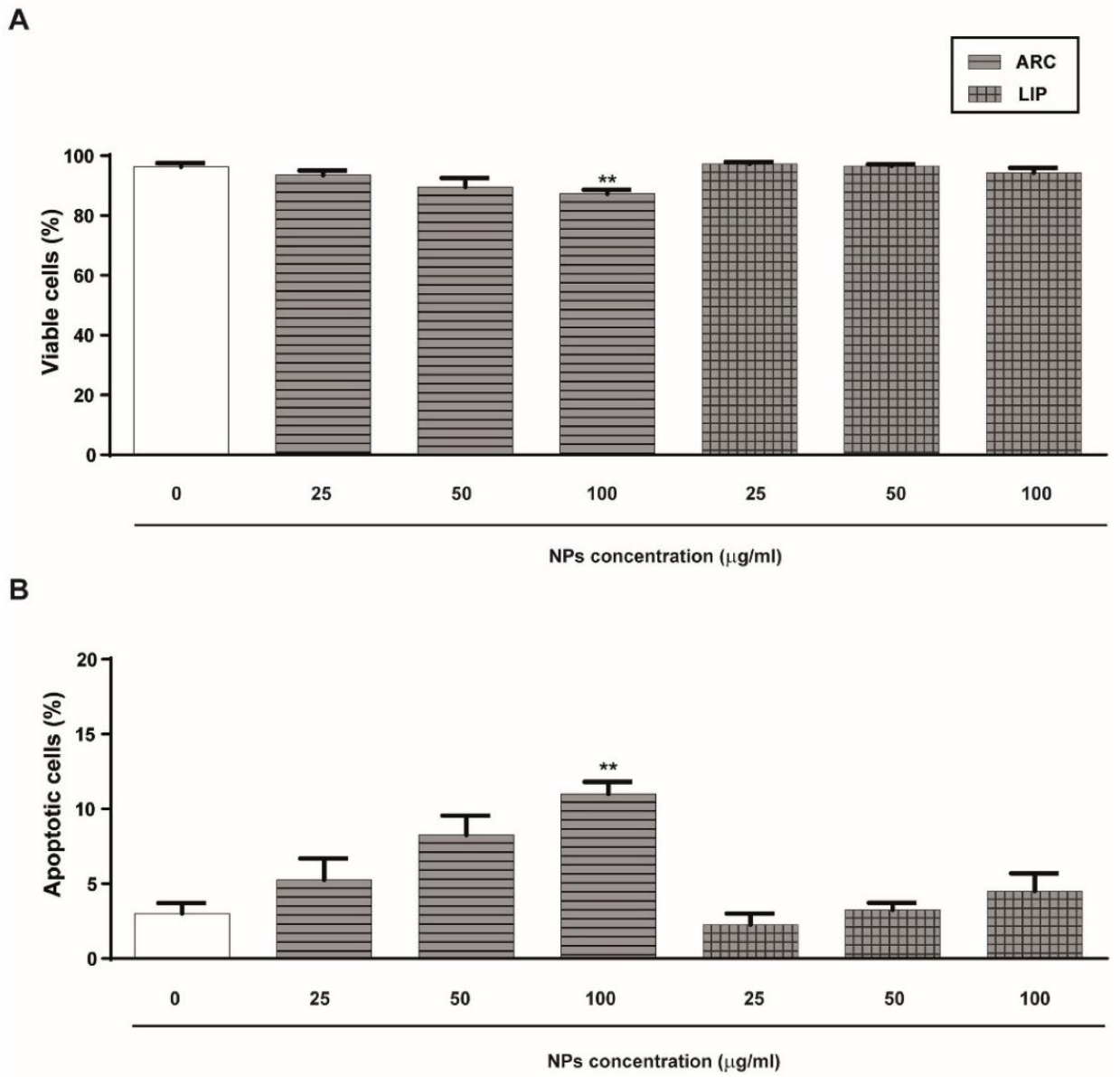

Figure 1. *Cont.*

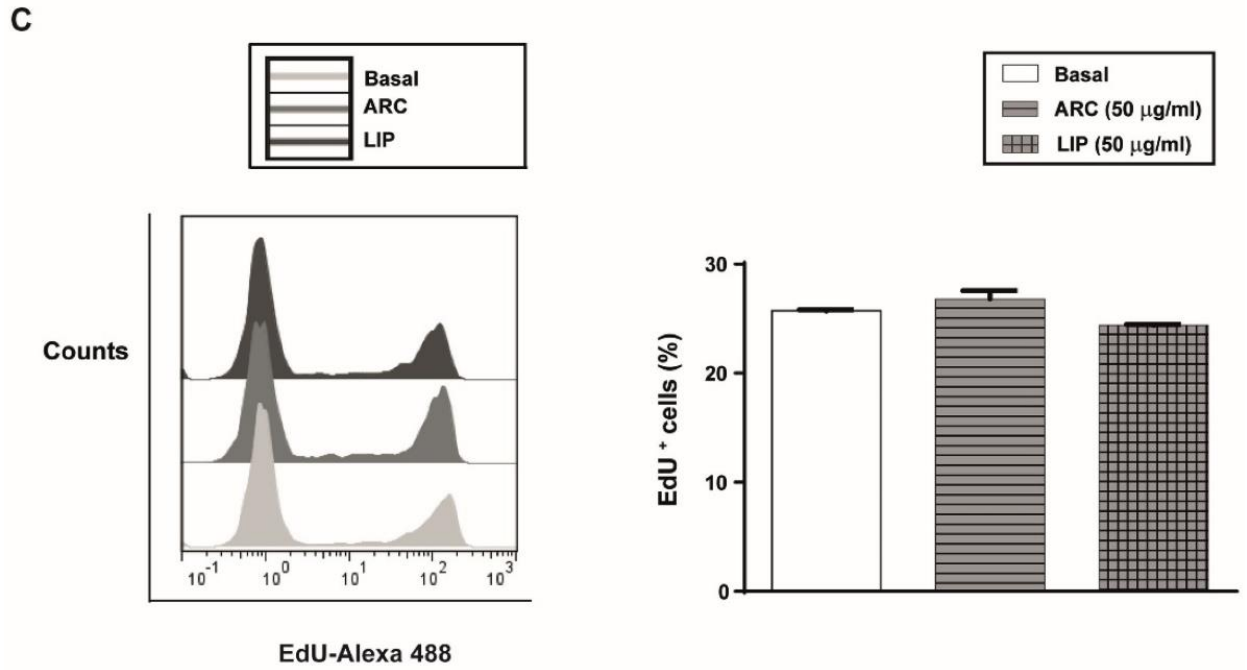

Figure 1. ARC do not alter HUVEC's viability or proliferation. HUVEC were incubated for 24 h in the absence or presence of nanoarchaeosomes (ARC) or liposomes (LIP) at different concentrations. The percentage of viable cells (**A**) and apoptotic cells (**B**) was determined by staining cells with acridine orange and ethidium bromide (100 μg/mL) (one-way ANOVA followed by the Bonferroni multiple comparison tests; ** $p < 0.01$ vs. Basal. (**C**) The percentage of proliferating cells was determined after 24 h by measuring EdU incorporation in the viable subpopulation by flow cytometry. Results are the mean ± SEM of four to five independent experiments.

3.3. ARC Selectively Inhibit the Expression of E-Selectin and ICAM-1

We next investigated the effect of ARC on different endothelial cell inflammatory and hemostatic responses. Figure 2A shows that basal expression levels of the cell adhesion molecules, E-selectin and ICAM-1, were not modified by the presence of ARC. However, exposure of endothelial cells to ARC reduced the levels of E-selectin or ICAM-1 expression triggered by LPS, Pam3CSK4, or *E coli* (Figure 2B–D). ARC inhibited ICAM-1 expression in *E.coli* stimulated cells with an IC50 = 9.9 ± 1.91 μg/mL. Intriguingly, E-selectin and ICAM-1 expression levels in TNF-α or IL-1β stimulated cells were not modified by the ARC (Figure 2E,F). On the other hand, the expression of both endothelial cell adhesion molecules induced by any stimuli (Figure 2B–F) was similar regardless of their exposure or not to liposomes. A decreased expression of ICAM-1 mediated by ARC was also observed when HMEC were used instead of HUVEC (Supplementary Figure S2A). Moreover, qPCR studies showed that the inhibitory effect was associated with a significant reduction in the mRNA levels (Supplementary Figure S2B).

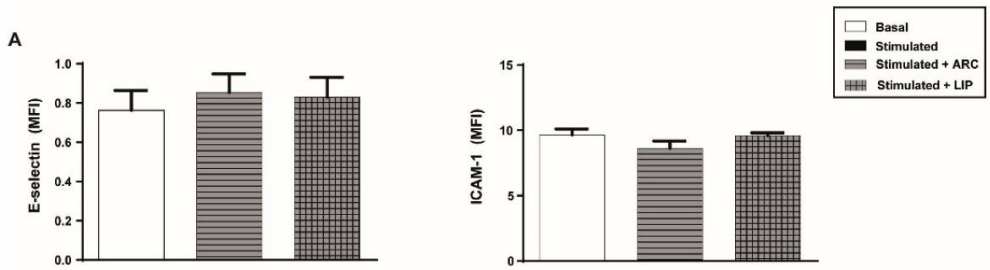

Figure 2. *Cont.*

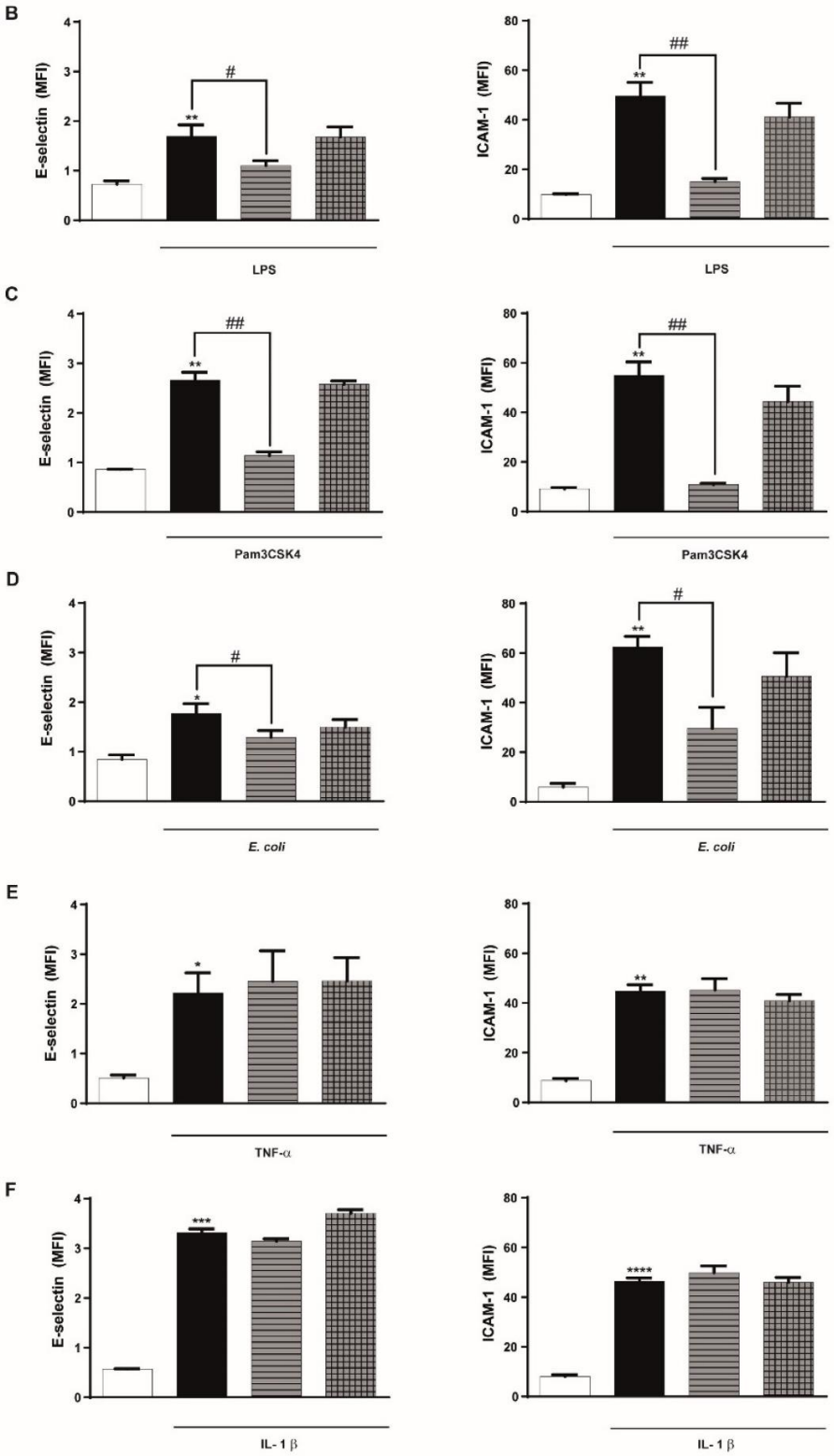

Figure 2. ARC selectively inhibit the expression of E-selectin and ICAM-1 on stimulated endothelial cells. HUVEC were treated or not with nanoarchaeosomes (ARC) or liposomes (LIP) (**A**). HUVEC were incubated with nanoarchaeosomes (ARC) or liposomes (LIP) at a concentration of 50 μg/mL and stimulated with (**B**) LPS (1 μg/mL); (**C**) Pam3CSK4 (1 μg/mL); (**D**) *E. coli* (MOI = 0.01); (**E**) TNF-α (0.3 μg/mL) or (**F**) IL-1β (0.1 ng/mL) Expression of E-selectin and ICAM-1 was evaluated 4 and 18 h after-stimulation, respectively (one-way ANOVA followed by Bonferroni multiple comparisons test); * $p < 0.05$, ** $p < 0.01$, *** $p < 0.001$ and **** $p < 0.0001$ vs. basal; # $p < 0.05$ and ## $p < 0.01$ between labeled groups. Results are the mean ± SEM of four to five independent experiments.

3.4. ARC Decrease the Levels of Cytokines Released by Endothelial Cells Stimulated with LPS or Pam3CSK4 but Not with TNF-α or IL-1β

Having demonstrated an inhibitory effect of ARC on endothelial cell adhesion molecules expression, we next evaluated the effect of ARC on the production of pro-inflammatory IL-6. As it is shown in Figure 3A,B, IL-6 released by LPS or Pam3CSK4 was significantly decreased by the presence of ARC but not by liposomes. However, and similarly to the results obtained in the expression of cell adhesion molecules, ARC did not modify IL-6 secretion triggered by TNF-α or IL-1β (Figure 3C,D).

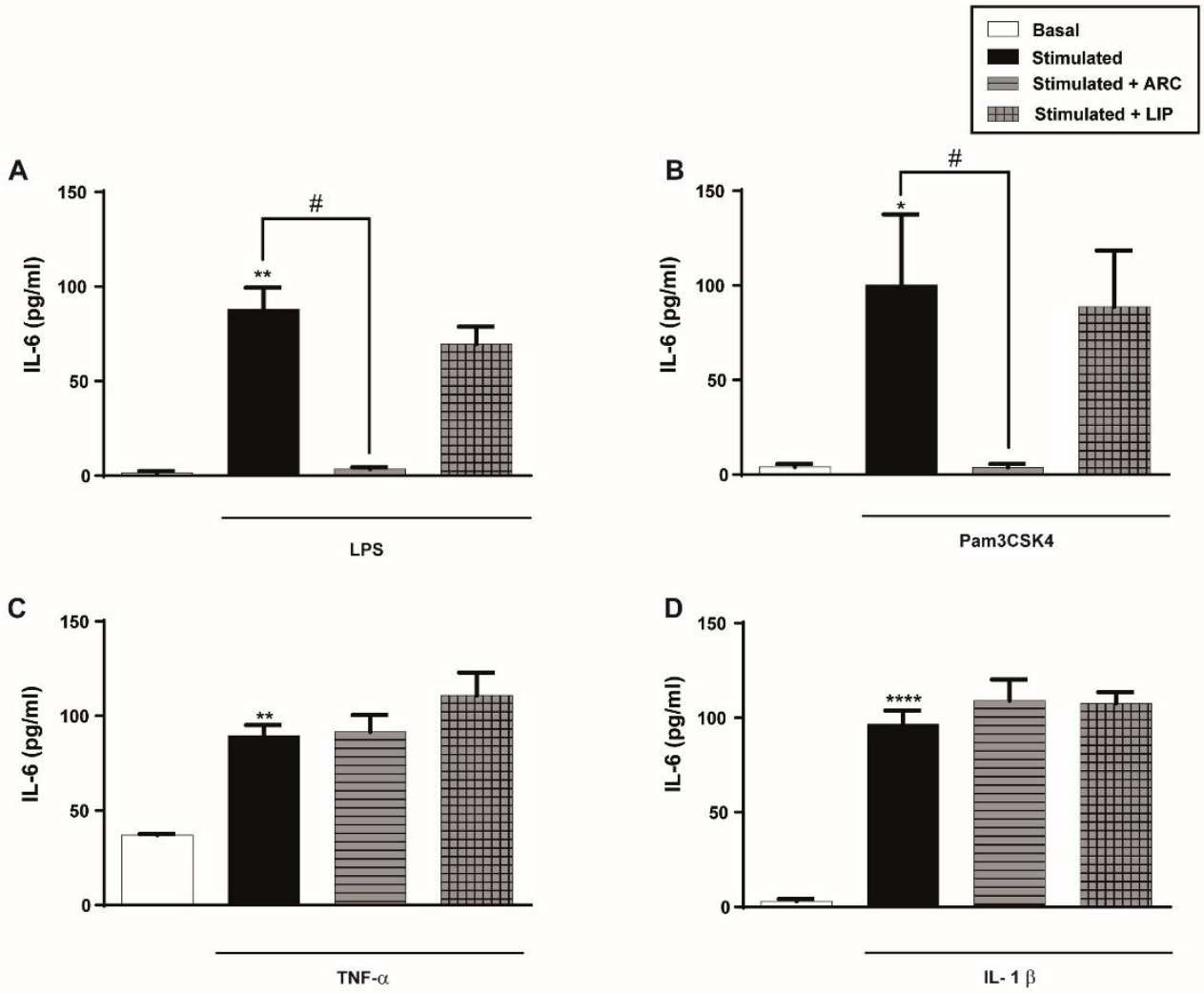

Figure 3. ARC selectively decrease the release of IL-6 by stimulated endothelial cells. HUVEC were stimulated with (**A**) LPS (1 μg/mL); (**B**) Pam3CSK4 (1 μg/mL); (**C**) TNF-α (3 ng/mL) or (**D**) IL-1β (0.1 ng/mL) and incubated with nanoarchaeosomes (ARC) or liposomes (LIP) at a concentration of 50 μg/mL for 18 h. Concentrations of IL-6 in supernatants were determined by ELISA (one-way ANOVA followed by a Bonferroni multiple comparisons test; * $p < 0.05$, ** $p < 0.01$ and **** $p < 0.0001$ versus basal; # $p < 0.05$ between labeled groups). Results are the mean ± SEM of four to five independent experiments.

3.5. The Inhibitory Effect of ARC Is Not Due to Their Interaction with LPS, Pam3CSK4, or E. coli or Their Receptors

The observation that ARC inhibited endothelial cell activation by LPS, Pam3CSK4, or *E. coli* but not by TNF-α or IL-1β raised the question of whether there was an interaction between these stimuli and/or their receptors and whether ARC could lead to the inhibition of the agonist's activity. Hence, HUVEC were pre-incubated with ARC for 1 h, then the

medium was removed, the cells were washed and then stimulated for 18 h. Figure 4A–D shows that even under these experimental conditions, ICAM-1 expression triggered by LPS, Pam3CSK4, or *E. coli* but not TNF-α stimulated cells was reduced by ARC and not by liposomes. Moreover, we also observed that the augmentation of ICAM-1 or IL-6 levels triggered by activation of HUVEC with Poly (I: C), an agonist of endosomal TLR3, or by the combination of PMA plus Ionomycin, receptor-independent agonists, was also blocked by the presence of ARC (Supplementary Figure S3A,B).

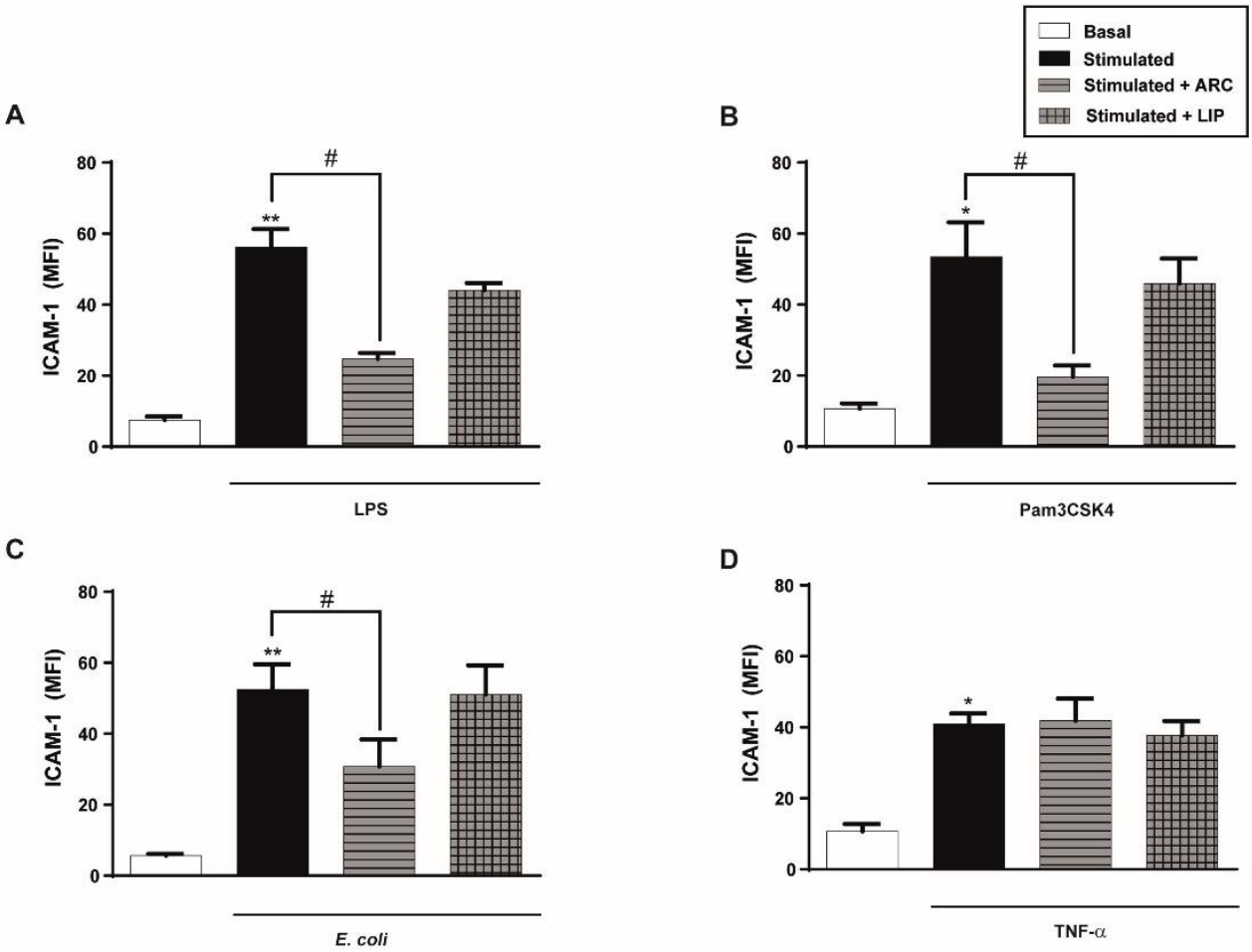

Figure 4. Preincubation with ARC also selectively inhibits ICAM-1 expression of endothelial cells. HUVEC were preincubated with nanovesicles (50 μg/mL) for 1 h, then washed and cells were stimulated with (**A**) LPS (1 μg/mL); (**B**) Pam3CSK4 (1 μg/mL); (**C**) *E. coli* (MOI = 0.01) or (**D**) TNF-α (0.3 ng/mL). ICAM-1 expression was evaluated 18 h poststimulation. (one-way ANOVA followed by Bonferroni multiple comparisons test; * $p < 0.05$ and ** $p < 0.01$ vs. basal; # $p < 0.05$ between labeled groups). Results are the mean ± SEM of 4 to 5 independent experiments.

3.6. ARC Decrease the Levels of vWF Released by Stimulated HUVEC

To determine whether ARC were also capable of reducing the prothrombotic activity of endothelial cells, we next examined its effect on two secretory pathways of vWF. vWF can be constitutively released during synthesis, or secreted from Weibel-Palade bodies (WPBs) in a regulated manner in response to various stimuli [40]. We found that the basal levels (Figure 5A) and the increased amount of vWF-triggered by LPS or Pam3CSK4 were markedly reduced by ARC (Figure 5B,C). Notably, similar results were obtained when cells were stimulated with TNF-α or IL-1β (Figure 5D,E). The reduction in vWF levels was also observed at the mRNA expression (Supplementary Figure S4A,B). Neither the release nor the synthesis of vWF was modified by the liposomes (Figure 5A–E).

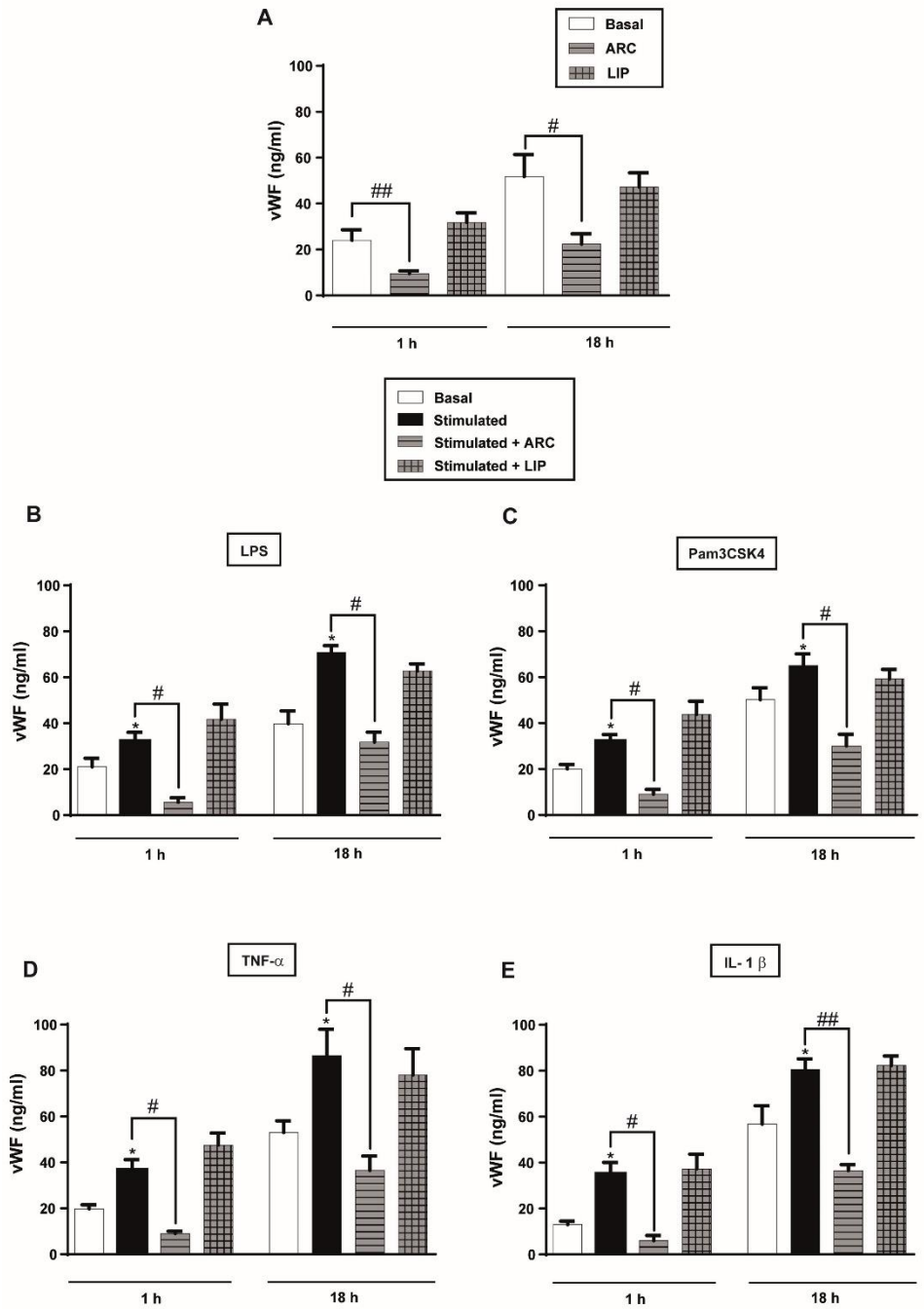

Figure 5. ARC decreases the amount of vWF released by endothelial cells. HUVEC were (**A**) unstimulated or stimulated with (**B**) LPS (1 μg/mL); (**C**) Pam3CSK4 (1 μg/mL); (**D**) TNF-α (3 ng/mL) or (**E**) IL-1β (1 ng/mL) and incubated with nanoarchaeosomes (ARC) or liposomes (LIP) at a concentration of 50 μg/mL for 1 and 18 h. The vWF concentrations in the supernatants were determined by ELISA (one-way ANOVA followed by Bonferroni multiple comparisons test; * $p < 0.05$ vs. basal; # $p < 0.05$ and ## $p < 0.01$ between the labeled groups). Results are the mean ± SEM of four to five independent experiments.

3.7. ARC Are Internalized by HUVEC

Considering that the effect of nanovesicles is generally determined in part by how they are processed by cells, we decided to investigate the fate of ARC during their interaction with the endothelial cells. Hence, we used RhPE-labeled ARC for visualization and quantitative analysis of cellular uptake of the nanovesicles. The extent of uptake by cells was significantly higher for ARC than for liposomes at different times, and the

maximum uptake efficiency occurred at 18 h (Figure 6A). By using confocal microscopy, we observed a high amount of RhPE-labeled ARC inside the cells while liposomes were poorly internalized (Figure 6B). The extent of the uptake was not modified in the presence of a stimulus (Supplementary Figure S5).

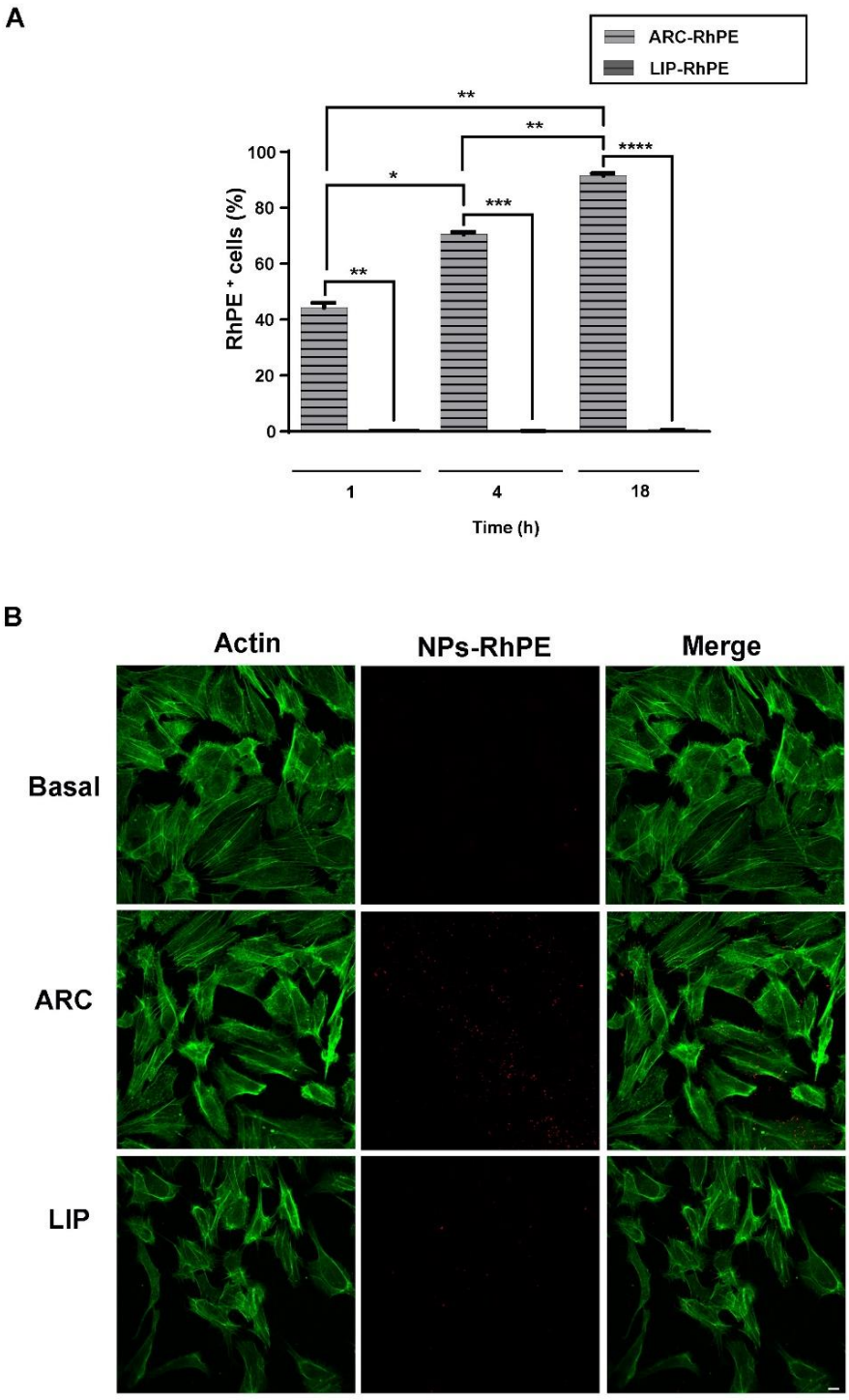

Figure 6. ARC are internalized by HUVEC. HUVEC were incubated for 1, 4 and 18 h with RhPE-labeled nanovesicles (ARC-RhPE and LIP-RhPE). Uptake assays were performed by (**A**) flow cytometry (one-way ANOVA followed by Bonferroni multiple comparisons test; * $p < 0.05$, ** $p < 0.01$, *** $p < 0.01$ and **** $p < 0.001$ between the labeled groups) and (**B**) Confocal microscopy. Representative images show RhPE-nanovesicles (red) and cytoplasm (green, FITC-phalloidin staining). Scale bars: 10 μm.

3.8. ARC Attenuate LPS-Induced Activation of NF-κB Pathway

MAPK and NF-κB signaling are involved in the inflammatory response of HUVEC, including the expression of chemokines, cytokines, and adhesion molecules [41]. To understand the signaling pathway involved in the anti-inflammatory activity of ARC we analyzed the activation of the NF-κB pathway through IκBα degradation and phosphorylation of ERK1/2. Flow cytometry and Western blotting studies showed that phosphorylation of ERK1/2 induced by LPS was attenuated in the presence of ARC (Figure 7A,B). The IκBα degradation by LPS was also inhibited by ARC (Figure 7C) indicating that ARC modulate the inflammatory response in LPS-stimulated HMEC through NF-κB and the ERK1/2 signaling pathway. Neither phosphorylation of ERK nor IκBα degradation mediated by LPS were modified by liposomes (Figure 7A–C).

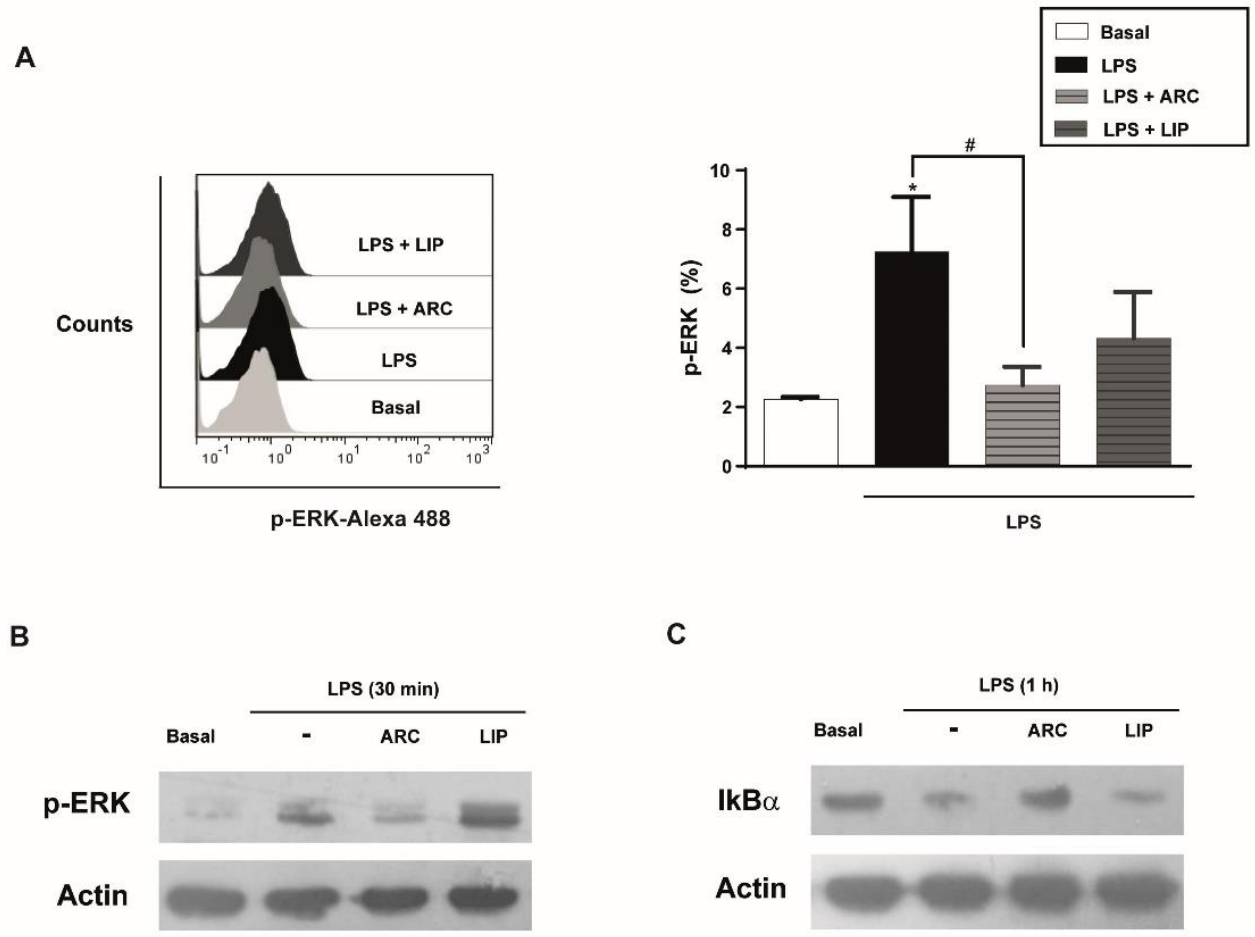

Figure 7. ARC attenuate LPS-induced phosphorylation of extracellular signal-regulated kinase (ERK1/2) and activation of NF-κB pathway in endothelial cells. (**A**) HMEC were stimulated with LPS (1 μg/mL) in the absence or presence of nanovesicles for 30 min, labeled with anti-p-ERK and analyzed by flow cytometry (one-way ANOVA followed by Bonferroni multiple comparisons test; * $p < 0.05$ vs. basal; # $p < 0.05$ between the labeled groups). HMEC were stimulated with LPS (1 μg/mL) in the absence or presence of nanoarchaeosomes (ARC) or liposomes (LIP) for 30 min (**B**) or 1 h (**C**) and cell extracts were analyzed by Western blot for p-ERK or IkBα, respectively. Representative images.

4. Discussion

A detailed comprehension of the processes and mechanisms underlying cellular NPs uptake is critical for exploring the effects of nanomaterials on biological systems. Moreover, evaluation of their potential harm to organisms is mandatory to promote a safer and more efficient application of nanomaterials in biomedical fields. In this study, we have

analyzed the effect of ARC from *H. tebenquichense* on the endothelium and compared it with conventional liposomes. We found that these ARC, up to 50 μg/mL, exert a very strong anti-inflammatory effect on endothelial cells without altering cell viability or proliferation. Exposure of HUVEC to ARC markedly inhibited the expression and synthesis of cell adhesion molecules (CAMs) such as E-selectin and ICAM-1, the release of IL-6, and vWF. None of these effects were observed when endothelial cells were treated with conventional liposomes constituted by hydrogenated soybean phospholipids. Most of the in-vitro studies show that biodegradable nanocarriers do not have a direct effect on the endothelium [42–44] or that NPs exert an opposite effect compared to ARC on the endothelium, which means that they are pro-inflammatory [45,46]. So far, there is no evidence showing that NPs per se can inhibit endothelial cell activation responses.

The inhibitory effect of ARC in all effector-endothelial responses evaluated, except on the release of vWF, was observed when cells were stimulated with LPS, *E. coli*, or Pam3CSK4 (the two former ligands of Toll-like receptor (TLR) 4 and the latter of TLR2) but not when they were activated by cytokines such as IL-1β or TNF-α.

Taking into account that the signaling in response to all stimuli investigated in the current study has been shown to share the same molecular signals downstream from their receptors [47–50], it could be speculated that the inhibitory effects of ARC were specifically acting at the level of the agonist receptor complex or first target signaling proteins. Interference with efficient TLR agonist signaling by ARC at the level of the ligand-receptor could occur by direct interaction with TLR or accessory molecules, and interference with the assembly of the TLR receptor complex. In this regard, it has been shown that oxidized phospholipids antagonize the pro-inflammatory response to LPS but not by TNF-α and IL-1β, and its protective effect was ascribed to the inhibition of LPS binding to the LPS binding protein and CD14, resulting in the suppression of TLR-dependent signaling pathways [51]. Similarly, high-density lipoprotein interferes with LPS activity caused by the competitive binding of the LPS–LBP–CD14 complex to apoAI [52–54]. However, in our experiments, when ARC were incubated for 1 h and then removed before stimulation of the cells with LPS, Pam3CSK4, or *E. coli*, the anti-inflammatory effect persisted. Moreover, the inhibitory effect of ARC was also observed when endothelial cells were stimulated with PMA and Ionomycin (two agonists acting independently of receptor interaction) or with Poly (I: C) a ligand of the endosomal TLR3. Altogether these data suggest that a direct interaction between ARC and specific ligands of TLRs, their receptors, or accessory molecules is unlikely.

Several recent reports indicate that lipid microdomains favor the recruitment and clustering of the TLR machinery. Upon activation, TLRs migrate to specific lipid microdomains together with co-receptors where they are recruited, activated, and able to transmit signals [55–57]. In this regard, the down-regulating effect of surfactants or oxidized phospholipids on LPS activation was correlated to a diminished TLR4 translocation into lipid rafts [58,59]. Different from liposome bilayers, ARC bilayers are highly disorganized but with low lateral mobility and high local microviscosity [60–62]. Two remarkable features of archaeolipids are their structural resemblance with ramified iso-stearic acid and the exhibition of solubilizing and fluidity properties of oleic acid [63], which allow ARC bilayers to partition poorly soluble drugs [23,29]. Recently, the ability of archaeolipids to establish strong non-covalent bonds with cholesterol derivatives has been described [64]. Since we demonstrated that ARC are endocytosed, it could be conceivable that upon endocytosis, ARC downregulate endothelial activation responses induced by TLRs agonists by partitioning into the cell bilayer, sequestering cholesterol, and disrupting lipid rafts. This may be a relevant mechanism by which several lipid structures can modulate cellular responses.

PMA, on the other hand, is a phorbol ester that does not require receptors to reversibly activate Protein kinase (PK) C, a pathway ending in NF-κB activation. The PCK activation depends on its partition on the surface of PMA containing bilayers [65]. Therefore, a possible mechanism for PMA plus Ionomycin inhibition could be that archaeolipids in

the cell membrane associate with the phorbol ester-binding domain of PKC, inhibiting its activation by PMA.

Finally, despite IL-1β and TNF-α signalling routes converging in NF-kB activation, the early events at the level of cell membrane differ from those that take place for TLRs. Upon ligand binding, IL-1β migrate into caveolae (flask-shaped invaginated microdomains rich in caveolin) instead of lipid rafts [66,67], whereas TNF-α mediated NF-kB activation, is reported to be independent of caveolae or lipid rafts [68]. Hence, the absence of anti-inflammatory effect upon IL-1β stimulation could be explained by a refractory character of caveolae to archaeolipid induced disorganization. On the other hand, because of its independence with early membrane events, the TNF-α stimuli would not be affected by archaeolipids.

Future experiments are necessary to elucidate the molecular basis of the agonist-selective-inhibitory effect of ARC on endothelial activation responses.

Induction of CAMs as well as the release of pro-inflammatory cytokines are controlled at the level of gene transcription and requires among the different molecular signals the binding of the transcription factor NF-kB to the regulatory region within the promoters of each of these genes [69]. Our data show that the inhibition of both NF-kB pathway activation and ERK phosphorylation are involved in the anti-inflammatory effect mediated by ARC. The role of NF-kB appears to be of major relevance not only to these ARC but also to the different NPs, such as those that are pro-inflammatory, that exert this effect through activation of this pathway.

Besides reducing the expression of CAMs and the release of cytokines, ARC markedly impaired the release and synthesis of vWF. The inhibitory effect was observed both in the acute and the constitutive release of vWF induced by all agonists tested. Since WPBs degranulation involves the rearrangement of cytoskeletal actin and myosin microfilaments, it could be possible that ARC interfere not only with lipid rafts assembly but also with cytoskeletal rearrangement. In this regard, it was reported that treatment of HUVEC with the anti-inflammatory lipid molecules such as eicosapentaenoic or docosahexaenoic acid impairs the release of vWF by attenuating acting reorganization [70]. WPBs are endothelial storage granules of vWF and other vasoactive molecules such as P-selectin and endothelin-1. Because the excessive secretion of these molecules contributes to inflammation related to hypertension and thrombosis, the blockade of WPBs exocytosis is critical to lessen endothelial dysfunction. The central role of vWF in thrombosis has made it a promising target for research into new antiplatelet therapies that inhibit vWF. It has been suggested that directly limiting vWF release from WPBs has the potential as a therapeutic for cardiovascular disease [71]. In addition, the expression of CAMs, as well as the release of IL-6 or IL-1β from endothelial cells, represents one of the earliest pathological changes in immune and inflammatory diseases such as atherosclerosis [72].

5. Conclusions

The use of nanoparticulate carriers in biomedicine is gaining popularity due to their ability to deliver drugs to specific biological targets, thereby addressing unmet medical and pharmaceutical needs. Our data demonstrate for the first time the important ability of ARC to significantly reduce endothelial cell activation and vWF release and suggest that its exploration in vasculopathies may be of particular interest.

Supplementary Materials: The following supporting information can be downloaded at: https://www.mdpi.com/article/10.3390/pharmaceutics14040736/s1. Table S1: List of Primers sequences; Figure S1: ESI-MS of TPL from *H. tebenquichense*; Figure S2: ARC selectively inhibit the protein and mRNA expression level of ICAM-1 on stimulated endothelial cells; Figure S3: ARC inhibit the expression of ICAM-1 and secretion of IL-6 on stimulated endothelial cells; Figure S4: ARC inhibit the mRNA expression level of vWF on stimulated endothelial cells; Figure S5: ARC are internalized by stimulated HUVEC.

Author Contributions: Conceptualization, E.L.R. and M.S.; Data curation, N.C.; Formal analysis, N.C.; Funding acquisition, E.L.R. and M.S.; Investigation, E.L.R. and M.S.; Methodology, N.C. and H.J.; Project administration, E.L.R. and M.S.; Resources, H.J. and S.T.; Software, N.C.; Supervision, E.L.R. and M.S.; Validation, N.C., E.L.R. and M.S.; Visualization, N.C. and M.S.; Writing—original draft, N.C.; Writing—review & editing, S.T., E.L.R. and M.S. All authors have read and agreed to the published version of the manuscript.

Funding: This research was funded by (PICTs 2016/1470, 2017/1188 and 2019/02307) from the National Agency for Scientific and Technological Promotion (ANPCyT), Argentina to MS and Research Secretary from the University of Quilmes to ER. The APC was funded by PICT 2019/02307 from the National Agency for Scientific and Technological Promotion (ANPCyT) Argentina to MS and Research Secretary from the University of Quilmes to ER.

Institutional Review Board Statement: The study was conducted in accordance with the Declaration of Helsinki, and approved by the Institutional Ethics Committee of National Academy of Medicine, Argentina (protocol code: 6/21/CEIANM and date of approval: 3 March 2021) for studies involving humans.

Informed Consent Statement: Informed consent was obtained from all subjects involved in the study.

Data Availability Statement: Not applicable.

Conflicts of Interest: The authors declare that they have no conflict of interest. The funders had no role in the design of the study; in the collection, analyses, or interpretation of data; in the writing of the manuscript, or in the decision to publish the results.

References

1. Younis, M.A.; Tawfeek, H.M.; Abdellatif, A.A.H.; Abdel-Aleem, J.A.; Harashima, H. Clinical Translation of Nanomedicines: Challenges, Opportunities, and Keys. *Adv. Drug Deliv. Rev.* **2022**, *181*, 114083. [CrossRef] [PubMed]
2. Guo, P.; Huang, J.; Moses, M.A. Cancer Nanomedicines in an Evolving Oncology Landscape. *Trends Pharmacol. Sci.* **2020**, *41*, 730–742. [CrossRef] [PubMed]
3. US Food and Drug Administration. *FDA Approves First-of-Its Kind Targeted RNA-Based Therapy to Treat a Rare Disease*; US Food and Drug Administration: Silver Spring, MD, USA, 2018.
4. Suzuki, Y.; Ishihara, H. Difference in the Lipid Nanoparticle Technology Employed in Three Approved SiRNA (Patisiran) and MRNA (COVID-19 Vaccine) Drugs. *Drug Metab. Pharmacokinet.* **2021**, *41*, 100424. [CrossRef] [PubMed]
5. WHO. *Cardiovascular Diseases (CVDs)*; WHO: Geneva, Switzerland, 2019.
6. Wang, D.K.; Rahimi, M.; Filgueira, C.S. Nanotechnology Applications for Cardiovascular Disease Treatment: Current and Future Perspectives. *Nanomed. Nanotechnol. Biol. Med.* **2021**, *34*, 102387. [CrossRef] [PubMed]
7. Cicha, I. The Grand Challenges in Cardiovascular Drug Delivery. *Front. Drug Deliv.* **2021**, *1*, 1–4. [CrossRef]
8. Wolinsky, H. A Proposal Linking Clearance of Circulating Lipoproteins to Tissue Metabolic Activity as a Basis for Understanding Atherogenesis. *Circ. Res.* **1980**, *47*, 301–311. [CrossRef]
9. Gimbrone, M.A., Jr.; García-Cardeña, G. Endothelial Cell Dysfunction and the Pathobiology of Atherosclerosis. *Circ. Res.* **2016**, *176*, 139–148. [CrossRef]
10. Liu, X.; Sun, J. Endothelial Cells Dysfunction Induced by Silica Nanoparticles through Oxidative Stress via JNK/P53 and NF-KB Pathways. *Biomaterials* **2010**, *31*, 8198–8209. [CrossRef]
11. Tsou, T.C.; Yeh, S.C.; Tsai, F.Y.; Lin, H.J.; Cheng, T.J.; Chao, H.R.; Tai, L.A. Zinc Oxide Particles Induce Inflammatory Responses in Vascular Endothelial Cells via NF-KB Signaling. *J. Hazard. Mater.* **2010**, *183*, 182–188. [CrossRef]
12. Shi, J.; Sun, X.; Lin, Y.; Zou, X.; Li, Z.; Liao, Y.; Du, M.; Zhang, H. Endothelial Cell Injury and Dysfunction Induced by Silver Nanoparticles through Oxidative Stress via IKK/NF-KB Pathways. *Biomaterials* **2014**, *35*, 6657–6666. [CrossRef]
13. Guo, C.; Xia, Y.; Niu, P.; Jiang, L.; Duan, J.; Yu, Y.; Zhou, X.; Li, Y.; Sun, Z. Silica Nanoparticles Induce Oxidative Stress, Inflammation, and Endothelial Dysfunction in Vitro via Activation of the MAPK/Nrf2 Pathway and Nuclear Factor-KB Signaling. *Int. J. Nanomed.* **2015**, *10*, 1463–1477. [CrossRef] [PubMed]
14. Younis, N.K.; Ghoubaira, J.A.; Bassil, E.P.; Tantawi, H.N.; Eid, A.H. Metal-Based Nanoparticles: Promising Tools for the Management of Cardiovascular Diseases. *Nanomed. Nanotechnol. Biol. Med.* **2021**, *36*, 102433. [CrossRef] [PubMed]
15. Glassman, P.M.; Myerson, J.W.; Ferguson, L.T.; Kiseleva, R.Y.; Shuvaev, V.V.; Brenner, J.S.; Muzykantov, V.R. Targeting Drug Delivery in the Vascular System: Focus on Endothelium. *Adv. Drug Deliv. Rev.* **2020**, *157*, 96–117. [CrossRef] [PubMed]
16. Ding, B.S.; Dziubla, T.; Shuvaev, V.V.; Muro, S.; Muzykantov, V.R. Advanced Drug Delivery Systems That Target the Vascular Endothelium. *Mol. Interv.* **2006**, *6*, 98–112. [CrossRef]
17. Bose, R.J.; Ha, K.; McCarthy, J.R. Bio-Inspired Nanomaterials as Novel Options for the Treatment of Cardiovascular Disease. *Drug Discov. Today* **2021**, *26*, 1200–1211. [CrossRef]

18. Benvegnu, T.; Lemiegre, L.; Cammas-Marion, S. New Generation of Liposomes Called Archaeosomes Based on Natural or Synthetic Archaeal Lipids as Innovative Formulations for Drug Delivery. *Recent Pat. Drug Deliv. Formul.* **2009**, *3*, 206–220. [CrossRef]
19. Gonzalez, R.O.; Higa, L.H.; Cutrullis, R.A.; Bilen, M.; Morelli, I.; Roncaglia, D.I.; Corral, R.S.; Morilla, M.J.; Petray, P.B.; Romero, E.L. Archaeosomes Made of Halorubrum Tebenquichense Total Polar Lipids: A New Source of Adjuvancy. *BMC Biotechnol.* **2009**, *9*, 71. [CrossRef]
20. Higa, L.H.; Corral, R.S.; José Morilla, M.; Romero, E.L.; Petray, P.B. Archaeosomes Display Immunoadjuvant Potential for a Vaccine against Chagas Disease. *Hum. Vaccines Immunother.* **2013**, *9*, 409–412. [CrossRef]
21. Kaur, G.; Garg, T.; Rath, G.; Goyal, A.K. Archaeosomes: An Excellent Carrier for Drug and Cell Delivery. *Drug Deliv.* **2016**, *23*, 2497–2512. [CrossRef]
22. Moghimipour, E.; Kargar, M.; Handali, S. Archaeosomes as Means of Nano-Drug Delivery. *Rev. Med. Microbiol.* **2014**, *25*, 40–45. [CrossRef]
23. Parra, F.L.; Caimi, A.T.; Altube, M.J.; Cargnelutti, D.E.; Vermeulen, M.E.; De Farias, M.A.; Morilla, M.J.; Romero, E.L. Make It Simple: (SR-A1 + TLR7) Macrophage Targeted NANOarchaeosomes. *Front. Bioeng. Biotechnol.* **2018**, *6*, 163. [CrossRef] [PubMed]
24. Kate, M. Chapter 9 Membrane Lipids of Archaea. *New Compr. Biochem.* **1993**, *26*, 261–295. [CrossRef]
25. Schilrreff, P.; Simioni, Y.R.; Jerez, H.E.; Caimi, A.T.; de Farias, M.A.; Villares Portugal, R.; Romero, E.L.; Morilla, M.J. Superoxide Dismutase in Nanoarchaeosomes for Targeted Delivery to Inflammatory Macrophages. *Colloids Surf. B Biointerfaces* **2019**, *179*, 479–487. [CrossRef] [PubMed]
26. Caimi, A.T.; Parra, F.; de Farias, M.A.; Portugal, R.V.; Perez, A.P.; Romero, E.L.; Morilla, M.J. Topical Vaccination with Super-Stable Ready to Use Nanovesicles. *Colloids Surf. B Biointerfaces* **2017**, *152*, 114–123. [CrossRef]
27. Altube, M.J.; Selzer, S.M.; De Farias, M.A.; Portugal, R.V.; Morilla, M.J.; Romero, E.L. Surviving Nebulization-Induced Stress: Dexamethasone in PH-Sensitive Archaeosomes. *Nanomedicine* **2016**, *11*, 2103–2117. [CrossRef]
28. Omri, A.; Agnew, B.J.; Patel, G.B. Short-Term Repeated-Dose Toxicity Profile of Archaeosomes Administered to Mice via Intravenous and Oral Routes. *Int. J. Toxicol.* **2003**, *22*, 9–23. [CrossRef]
29. Julia Altube, M.; Ivonne Caimi, L.; Huck-Iriart, C.; Jose Morilla, M.; Lilia Romero, E.; Rosaria Lauro, M. Pharmaceutics Reparation of an Inflamed Air-Liquid Interface Cultured A549 Cells with Nebulized Nanocurcumin. *Pharmaceutics* **2021**, *13*, 1331. [CrossRef]
30. Higa, L.H.; Jerez, H.E.; De Farias, M.A.; Portugal, R.V.; Romero, E.L.; Morilla, M.J. Ultra-Small Solid Archaeolipid Nanoparticles for Active Targeting to Macrophages of the Inflamed Mucosa. *Nanomedicine* **2017**, *12*, 1165–1175. [CrossRef]
31. Higa, L.H.; Schilrreff, P.; Perez, A.P.; Iriarte, M.A.; Roncaglia, D.I.; Morilla, M.J.; Romero, E.L. Ultradeformable Archaeosomes as New Topical Adjuvants. *Nanomed. Nanotechnol. Biol. Med.* **2012**, *8*, 1319–1328. [CrossRef]
32. Kates, M.; Kushwaha, S.C. Isoprenoids and Polar Lipids of Extreme Halophiles. In *Archaea, a Laboratory Manual: Halophiles*; DasSarma, S., Fleischmann, E.M., Eds.; Cold Spring Harbor Laboratory Press: Cold Spring Harbor, NY, USA, 1995; pp. 35–54.
33. Böttcher, C.J.F.; Van gent, C.M.; Pries, C. A Rapid and Sensitive Sub-Micro Phosphorus Determination. *Anal. Chim. Acta* **1961**, *24*, 203–204. [CrossRef]
34. Altube, M.J.; Cutro, A.; Bakas, L.; Morilla, M.J.; Disalvo, E.A.; Romero, E.L. Nebulizing Novel Multifunctional Nanovesicles: The Impact of Macrophage-Targeted-PH-Sensitive Archaeosomes on a Pulmonary Surfactant. *J. Mater. Chem. B* **2017**, *5*, 8083–8095. [CrossRef]
35. Jaffe, E.A.; Nachman, R.L.; Becker, C.G.; Minick, C.R. Culture of Human Endothelial Cells Derived from Umbilical Veins. Identification by Morphologic and Immunologic Criteria. *J. Clin. Investig.* **1973**, *52*, 2745–2756. [CrossRef] [PubMed]
36. Negrotto, S.; Malaver, E.; Alvarez, M.E.; Pacienza, N.; D'Atri, L.P.; Pozner, R.G.; Gómez, R.M.; Schattner, M. Aspirin and Salicylate Suppress Polymorphonuclear Apoptosis Delay Mediated by Proinflammatory Stimuli. *J. Pharmacol. Exp. Ther.* **2006**, *319*, 972–979. [CrossRef] [PubMed]
37. Scholz, D.; Devaux, B.; Hirche, A.; Pötzsch, B.; Kropp, B.; Schaper, W.; Schaper, J. Expression of Adhesion Molecules Is Specific and Time-Dependent in Cytokine-Stimulated Endothelial Cells in Culture. *Cell Tissue Res.* **1996**, *284*, 415–423. [CrossRef] [PubMed]
38. Boyle, E.M.; Sato, T.T.; Noel, R.F.; Verrier, E.D.; Pohlman, T.H. Transcriptional Arrest of the Human E-Selectin Gene. *J. Surg. Res.* **1999**, *82*, 194–200. [CrossRef]
39. Carestia, A.; Kaufman, T.; Rivadeneyra, L.; Landoni, V.I.; Pozner, R.G.; Negrotto, S.; D'Atri, L.P.; Gómez, R.M.; Schattner, M. Mediators and Molecular Pathways Involved in the Regulation of Neutrophil Extracellular Trap Formation Mediated by Activated Platelets. *J. Leukoc. Biol.* **2016**, *99*, 153–162. [CrossRef]
40. Nightingale, T.; Cutler, D. The Secretion of von Willebrand Factor from Endothelial Cells; an Increasingly Complicated Story. *J. Thromb. Haemost.* **2013**, *11*, 192–201. [CrossRef]
41. Joyce, D.E.; Grinnell, B.W. Recombinant Human Activated Protein C Attenuates the Inflammatory Response in Endothelium and Monocytes by Modulating Nuclear Factor-KB. *Crit. Care Med.* **2002**, *30*, S288–S293. [CrossRef]
42. Berdiaki, A.; Perisynaki, E.; Stratidakis, A.; Kulikov, P.P.; Kuskov, A.N.; Stivaktakis, P.; Henrich-Noack, P.; Luss, A.L.; Shtilman, M.M.; Tzanakakis, G.N.; et al. Assessment of Amphiphilic Poly- N-Vinylpyrrolidone Nanoparticles' Biocompatibility with Endothelial Cells in Vitro and Delivery of an Anti-Inflammatory Drug. *Mol. Pharm.* **2020**, *17*, 4212–4225. [CrossRef]
43. Beconcini, D.; Felice, F.; Zambito, Y.; Fabiano, A.; Piras, A.M.; Macedo, M.H.; Sarmento, B.; Di Stefano, R. Anti-Inflammatory Effect of Cherry Extract Loaded in Polymeric Nanoparticles: Relevance of Particle Internalization in Endothelial Cells. *Pharmaceutics* **2019**, *11*, 500. [CrossRef]

44. Subash-Babu, P.; Al-Saran, N.; Alshammari, G.M.; Naif Al-Harbi, L.; Hussain Alhussain, M.; Shamlan, G.; Abdulaziz AlSedairy, S.; Abdullah Alshatwi, A.; Tsim, K.; Alshammari, M.G.; et al. Evaluation of Biosafety, Antiobesity, and Endothelial Cells Proliferation Potential of Basil Seed Extract Loaded Organic Solid Lipid Nanoparticle. *Front. Pharmacol.* **2021**, *12*, 2419. [CrossRef] [PubMed]
45. Corbalan, J.J.; Medina, C.; Jacoby, A.; Malinski, T.; Radomski, M.W. Amorphous Silica Nanoparticles Trigger Nitric Oxide/Peroxynitrite Imbalance in Human Endothelial Cells: Inflammatory and Cytotoxic Effects. *Int. J. Nanomed.* **2011**, *6*, 2821–2835. [CrossRef]
46. Nagarajan, M.; Maadurshni, G.B.; Tharani, G.K.; Udhayakumar, I.; Kumar, G.; Mani, K.P.; Sivasubramanian, J.; Manivannan, J. Exposure to Zinc Oxide Nanoparticles (ZnO-NPs) Induces Cardiovascular Toxicity and Exacerbates Pathogenesis–Role of Oxidative Stress and MAPK Signaling. *Chem. Biol. Interact.* **2022**, *351*, 109719. [CrossRef] [PubMed]
47. Maschera, B.; Ray, K.; Burns, K.; Volpe, F. Overexpression of an Enzymically Inactive Interleukin-1-Receptor-Associated Kinase Activates Nuclear Factor-KB. *Biochem. J.* **1999**, *339*, 227–231. [CrossRef]
48. Zhang, F.X.; Kirschning, C.J.; Mancinelli, R.; Xu, X.P.; Jin, Y.; Faure, E.; Mantovani, A.; Rothe, M.; Muzio, M.; Arditi, M. Bacterial Lipopolysaccharide Activates Nuclear Factor-KB through Interleukin-1 Signaling Mediators in Cultured Human Dermal Endothelial Cells and Mononuclear Phagocytes. *J. Biol. Chem.* **1999**, *274*, 7611–7614. [CrossRef]
49. Zhang, G.; Ghosh, S. Toll-like Receptor-Mediated NF-KB Activation: A Phylogenetically Conserved Paradigm in Innate Immunity. *J. Clin. Investig.* **2001**, *107*, 13–19. [CrossRef]
50. Martin, M.U.; Wesche, H. Summary and Comparison of the Signaling Mechanisms of the Toll/Interleukin-1 Receptor Family. *Biochim. Biophys. Acta-Mol. Cell Res.* **2002**, *1592*, 265–280. [CrossRef]
51. Bochkov, V.N.; Kadl, A.; Huber, J.; Gruber, F.; Binder, B.R.; Leitinger, N. Protective Role of Phospholipid Oxidation Products in Endotoxin-Induced Tissue Damage. *Nature* **2002**, *419*, 77–81. [CrossRef]
52. Wu, A.; Hinds, C.J.; Thiemermann, C. High-Density Lipoproteins in Sepsis and Septic Shock: Metabolism, Actions, and Therapeutic Applications. *Shock* **2004**, *21*, 210–221. [CrossRef]
53. Parker, T.S.; Levine, D.M.; Chang, J.C.C.; Laxer, J.; Coffin, C.C.; Rubin, A.L. Reconstituted High-Density Lipoprotein Neutralizes Gram-Negative Bacterial Lipopolysaccharides in Human Whole Blood. *Infect. Immun.* **1995**, *63*, 253–258. [CrossRef]
54. Gupta, H.; Dai, L.; Datta, G.; Garber, D.W.; Grenett, H.; Li, Y.; Mishra, V.; Palgunachari, M.N.; Handattu, S.; Gianturco, S.H.; et al. Inhibition of Lipopolysaccharide-Induced Inflammatory Responses by an Apolipoprotein AI Mimetic Peptide. *Circ. Res.* **2005**, *97*, 236–243. [CrossRef] [PubMed]
55. Triantafilou, M.; Miyake, K.; Golenbock, D.T.; Triantafilou, K. Mediators of Innate Immune Recognition of Bacteria Concentrate in Lipid Rafts and Facilitate Lipopolysaccharide-Induced Cell Activation. *J. Cell Sci.* **2002**, *115*, 2603–2611. [CrossRef] [PubMed]
56. Triantafilou, M.; Gamper, F.G.J.; Haston, R.M.; Mouratis, M.A.; Morath, S.; Hartung, T.; Triantafilou, K. Membrane Sorting of Toll-like Receptor (TLR)-2/6 and TLR2/1 Heterodimers at the Cell Surface Determines Heterotypic Associations with CD36 and Intracellular Targeting. *J. Biol. Chem.* **2006**, *281*, 31002–31011. [CrossRef] [PubMed]
57. McGettrick, A.F.; Brint, E.K.; Palsson-McDermott, E.M.; Rowe, D.C.; Golenbock, D.T.; Gay, N.J.; Fitzgerald, K.A.; O'Neill, L.A.J. Trif-Related Adapter Molecule Is Phosphorylated by PKCε during Toll-like Receptor 4 Signaling. *Proc. Natl. Acad. Sci. USA* **2006**, *103*, 9196–9201. [CrossRef]
58. Abate, W.; Alghaithy, A.A.; Parton, J.; Jones, K.P.; Jackson, S.K. Surfactant Lipids Regulate LPS-Induced Interleukin-8 Production in A549 Lung Epithelial Cells by Inhibiting Translocation of TLR4 into Lipid Raft Domains. *J. Lipid Res.* **2010**, *51*, 334–344. [CrossRef]
59. Walton, K.A.; Hsieh, X.; Gharavi, N.; Wang, S.; Wang, G.; Yeh, M.; Cole, A.L.; Berliner, J.A. Receptors Involved in the Oxidized 1-Palmitoyl-2-Arachidonoyl-Sn-Glycero-3-Phosphorylcholine-Mediated Synthesis of Interleukin-8: A Role for Toll-like Receptor 4 and a Glycosylphosphatidylinositol-Anchored Protein. *J. Biol. Chem.* **2003**, *278*, 29661–29666. [CrossRef]
60. Yamauchi, K.; Doi, K.; Yoshida, Y.; Kinoshita, M. Archaebacterial Lipids: Highly Proton-Impermeable Membranes from 1,2-Diphytanyl-Sn-Glycero-3-Phosphocoline. *BBA-Biomembranes* **1993**, *1146*, 178–182. [CrossRef]
61. Róg, T.; Vattulainen, I.; Bunker, A.; Karttunen, M. Glycolipid Membranes through Atomistic Simulations: Effect of Glucose and Galactose Head Groups on Lipid Bilayer Properties. *J. Phys. Chem. B* **2007**, *111*, 10146–10154. [CrossRef]
62. Kitano, T.; Onoue, T.; Yamauchi, K. Archaeal Lipids Forming a Low Energy-Surface on Air-Water Interface. *Chem. Phys. Lipids* **2003**, *126*, 225–232. [CrossRef]
63. Chollet, J.L.; Jozwiakowski, M.J.; Phares, K.R.; Reiter, M.J.; Roddy, P.J.; Schultz, H.J.; Ta, Q.V.; Tomai, M.A. Development of a Topically Active Imiquimod Formulation. *Pharm. Dev. Technol.* **1999**, *4*, 35–43. [CrossRef]
64. Carrer, D.C.; Higa, L.H.; Tesoriero, M.V.D.; Morilla, M.J.; Roncaglia, D.I.; Romero, E.L. Structural Features of Ultradeformable Archaeosomes for Topical Delivery of Ovalbumin. *Colloids Surf. B Biointerfaces* **2014**, *121*, 281–289. [CrossRef] [PubMed]
65. Mosior, M.; Newton, A.C. Mechanism of Interaction of Protein Kinase C with Phorbol Esters. *J. Biol. Chem.* **1995**, *270*, 25526–25533. [CrossRef]
66. Galbiati, F.; Razani, B.; Lisanti, M.P. Emerging Themes in Lipid Rafts and Caveolae. *Cell* **2001**, *106*, 403–411. [CrossRef]
67. Oakley, F.O.; Smith, R.L.; Engelhardt, J.F. Lipid Rafts and Caveolin-1 Coordinate Interleukin-1β (IL-1β)-Dependent Activation of NFκB by Controlling Endocytosis of Nox2 and IL-1β Receptor 1 from the Plasma Membrane. *J. Biol. Chem.* **2009**, *284*, 33255–33264. [CrossRef] [PubMed]
68. Doan, J.E.S.; Windmiller, D.A.; Riches, D.W.H. Differential Regulation of TNF-R1 Signaling: Lipid Raft Dependency of P42 Mapk/Erk2 Activation, but Not NF-KB Activation. *J. Immunol.* **2004**, *172*, 7654–7660. [CrossRef] [PubMed]

69. Collins, T.; Read, M.A.; Neish, A.S.; Whitley, M.Z.; Thanos, D.; Maniatis, T. Transcriptional Regulation of Endothelial Cell Adhesion Molecules: NF-κB and Cytokine-inducible Enhancers. *FASEB J.* **1995**, *9*, 899–909. [CrossRef] [PubMed]
70. Bürgin-Maunder, C.S.; Brooks, P.R.; Russell, F.D. Omega-3 Fatty Acids Modulate Weibel-Palade Body Degranulation and Actin Cytoskeleton Rearrangement in PMA-Stimulated Human Umbilical Vein Endothelial Cells. *Mar. Drugs* **2013**, *11*, 4435–4450. [CrossRef]
71. El-Mansi, S.; Nightingale, T.D. Emerging Mechanisms to Modulate VWF Release from Endothelial Cells. *Int. J. Biochem. Cell Biol.* **2021**, *131*, 105900. [CrossRef]
72. Springer, T.A.; Cybulsky, M.I. Traffic Signals on Endothelium for Leukocytes in Health, Inflammation, and Atherosclerosis. In *Atherosclerosis and Coronary Artery Disease*; Lippincott-Raven Publishers: Philadelphia, PA, USA, 1995; pp. 511–537.